Deciphering the role of TNF-α-induced protein 8-like 2 in the pathogenesis of necrotizing enterocolitis in neonatal rats

JUAN LUO[1], SHENGLIN YU[1], JIALONG XU[2], XIAOGANG SUN[2] and RUOYI WANG[2]

[1]Department of Neonatology, Children's Hospital of Soochow University, Suzhou, Jiangsu 215003; [2]Department of Pediatric Surgery, The Second Hospital of Shandong University, Jinan, Shandong 250033, P.R. China

Received August 11, 2022; Accepted June 23, 2023

DOI: 10.3892/etm.2023.12142

Abstract. Neonatal necrotizing enterocolitis (NNEC) is a disease characterized by intestinal inflammation and ischemic necrosis. Despite progress having been made during decades of research, details regarding its pathophysiology remain to be elucidated. It is known that abnormal expressions of TNF-α-induced protein 8-like 2 (TIPE2) can be observed in several diseases. However, the expression of TIPE2 in necrotizing enterocolitis (NEC) rats has not been examined before. The present study aimed to describe the expression pattern of TIPE2 and its role in NNEC pathogenesis. An NEC rat model was generated and used in the present study. All rats were sacrificed when the phenotype developed and the intestine between the lower end of the duodenum and the ileocecal were collected for further study. Hematoxylin and eosin, and immunohistochemical staining, reverse transcription-quantitative PCR and western blotting analysis were used to examine the expression of TIPE2. The results showed that the average body weight was significantly decreased in the NEC group compared with the control group along with a significant decrease of TIPE2 expression. However, the expressions of phosphatidylinositol-3-kinase (PI3K) and serine/threonine kinase AKT were significantly increased in NEC rats. The correlation analysis showed that the expressions of TIPE2 and PI3K were negatively correlated with a correlation coefficient of -0.797. To further determine the association between TIPE2 and PI3K/AKT pathway, two groups of wild type Sprague Dawley rats were infected with recombinant adenovirus Ad-V and Ad-TIPE2 respectively. The results showed that the expression of TIPE2 was significantly increased among rats in the Ad-TIPE2-infected group (OE group) compared to the ones from the Ad-V-infected group (NC group). However, the mRNA and protein expressions of PI3K and AKT were significantly decreased in Ad-TIPE2-infected rates. The difference of each index between OE and NC groups was statistically significant. The present study showed that the expression of TIPE2 was downregulated in NEC rats. TIPE2 might be involved in the pathogenesis of NEC by activating the PI3K/Akt signaling pathway.

Correspondence to: Professor Shenglin Yu, Department of Neonatology, Children's Hospital of Soochow University, 92 Zhongnan Street, Suzhou, Jiangsu 215003, P.R. China
E-mail: wm1971@sina.com

Professor Ruoyi Wang, Department of Pediatric Surgery, The Second Hospital of Shandong University, 247 Beiyuan Street, Jinan, Shandong 250033, P.R. China
E-mail: wangruoyi1974@163.com

Abbreviations: H&E, hematoxylin and eosin; IHC, immunohisto-chemical; LPS, lipopolysaccharides; NNEC, neonatal necrotizing enterocolitis; PI3K, phosphatidylinositol-3-kinase; PMSF, phenylmethylsulfonyl fluoride; SD, Sprague Dawley; TIPE2, TNF-α-induced protein 8-like 2

Key words: neonatal necrotizing enterocolitis, TNF-α-induced protein 8-like 2, phosphatidylinositol-3-kinase, serine/threonine kinase AKT, pathophysiological process

Introduction

As an acute necrosis inflammatory bowel disease, neonatal necrotizing enterocolitis (NNEC) primarily affects preterm infants. An epidemiology study shows that it is the most common gastrointestinal emergency in the neonatal intensive care unit (1) and is characterized as a worldwide epidemic disease that accounts for significant neonatal mortality and morbidity (2,3). It has been estimated that the incidence of necrotizing enterocolitis (NEC) is 1-3 patients per 1,000 live births and ~90% of all cases occur in preterm infants. Despite advances in perinatal and neonatal care have been achieved in past decades, NEC remains a leading cause of morbidity and mortality in preterm infants, with mortality rates as high as 30% (4,5).

To the best of the authors' knowledge, several important factors including prematurity, intestinal immaturity, hypoxia-ischemia, colonization with pathogenic bacteria and formula feeding participate in bowel injury and intestinal inflammation. All the aforementioned factors can result in epithelial injury and intestinal tissue damage, including necrosis and apoptosis of intestinal tissue (6). However, a number of details regarding the pathogenesis of NEC remain to be elucidated.

Previous studies revealed that TIPE2 might promote tumor growth and progression. More specifically, Zhu *et al* (7) found that the expression of TIPE2 was reduced in gastric cancer

while Liu *et al* (8) demonstrated that TIPE2 is minimally expressed in human glioma tissues and cell lines. In inflammatory and autoimmune diseases, Wang *et al* (9) found that *Pseudomonas aeruginosa* infection could reduce expression of TIPE2 in mouse corneas. Zhou *et al* (10) demonstrated that the expression of TIPE2 was downregulated in a collagen-induced arthritis model, which was accompanied by the occurrence of arthritis. However, Lou *et al* (11) showed that TIPE2 deficiency reduced inflammatory responses in a murine acute colitis model by enhancing immune responses to commensal bacteria. Therefore conflicting results have been reported regarding the expression of TIPE2 in different diseases.

The phosphoinositide 3-kinases (PI3Ks) are a conserved family of signal transduction enzymes (12,13). PI3Ks and its downstream serine/threonine kinase AKT (also known as protein kinase B) serve important roles in regulating cell activation, inflammatory responses, chemotaxis and apoptosis (13). It has been proved that modulation of certain PI3K isoforms may elicit beneficial effects, while activating other PI3K isoforms may result in pathology changes (14).

In the present study, the expression of TIPE2 and PI3K/AKT pathway proteins were examined by using a rat model of NEC. Further mechanism study was conducted using wild type neonatal SD rats that were infected with recombinant adenovirus Ad-TIPE2.

Materials and methods

Animals. Neonatal Sprague Dawley (SD) rats (3 days old: 45 rats, 20 of which were used in the follow-up experiments; and 14 days old, 17 rats, 10 of which were used in the follow-up experiments) were obtained from the Animal Experiment Center of the Second Hospital of Shandong University. The ambient temperature was 22±3˚C, and the humidity was 40-80%. The 3-days-old rats were adapted in cages with a 12-h light/dark cycle for 2 days, The 14-days-old SD rats were randomly divided into two groups (OE group and NC group). After 3 days of normal feeding, rats in the OE group were transfected with TIPE2-overexpressing adenovirus, while rats in the NC group were transfected with NC virus. After 7 days of feeding under the same conditions, the rats were sacrificed for further experiments. The present study was approved by the Animal Experiment Center of the Second Hospital of Shandong University (Shandong, China; approval no. KYLL-2022LW103). All animal-related procedures complied with the Guide for the Care and Use of Laboratory Animals published by the National Institutes of Health (no. 85-23, revised 1996).

Main reagents and antibodies. Polyclonal antibodies against TIPE2 (cat. no. 15940-1-AP) and β-actin (dilution, 1:500; cat. no. Biotin-60008) were purchased from ProteinTech Group, Inc. Pan-AKT rabbit pAb (dilution, 1:1,000; cat. no. A18120) and phosphorylated (p-) AKT1-S473+AKT2-S474+AKT3-S472 rabbit mAbs (dilution, 1:1,000; cat. no. AP1208) were obtained from ABclonal Biotech Co., Ltd. Polyclonal antibodies against PI3-kinase p85α/γ (dilution, 1:1,000; cat. no. AP71896) and PI3-kinase p85α(p-Tyr607) (dilution, 1:1,000; cat. no. AP67697) were provided by Abcepta. HRP-conjugated secondary antibody (H+L) (cat. no. BL003A) and bovine serum albumin V (cat. no. BS114-100g) were obtained from Biosharp Life Sciences. RIPA lysate (tissue/cell, cat. no. R0020) [including phenylmethylsulfonyl fluoride (PMSF)] was purchased from Beijing Solarbio Science & Technology Co., Ltd. Phosphorylase inhibitor 100X (cat. no. SW105-02) and protease inhibitor cocktail 100X (cat. no. SW107-02) were obtained from Seven Biotech [Saiwen Innovation (Beijing) Biotechnology Co., Ltd.]. Tissue RNA Purification Kit Plus (cat. no. EN-RN002plus) was supplied by Yeasen Biotechnology (Shanghai) Co., Ltd. Evo M-MLV RT Kit with gDNA Clean for qPCR II (cat. no. AG11711) was provided by Accurate Biology. 2X Universal SYBR Green Fast qPCR Mix (cat. no. RK21203) was purchased from ABclonal Biotech Co., Ltd.

Experiment design and model establishment. The 3-day-old rats (weight 6-7 g) were randomly divided into two groups: i) Control group (control, n=10) without any intervention and ii) NEC group (NEC, n=10). The NEC model was established as described previously (15). Briefly, the NEC model was established by artificial feeding, hypoxia-cold stimulation and intraperitoneal injection of lipopolysaccharides (LPS). All animals were kept in specified facility with 28-30˚C and 45-65% humidity. Rats in the experimental group were artificially fed with the formula substitute of rat milk (16) [4.60 g infant formula, 8 g protein powder and 50 ml lipid emulsion (C14-24) every 100 ml] and 0.2 ml of the formula was given to each rat at every 4 h interval (q4h) within the first 24 h and 0.3 ml was given to each rat at q4h during 24-48 h while 0.4 ml was given to each rat at q4h for the last 24 h before experiment. NEC rats were placed in a box with pure nitrogen at 5 l/min for 7 min when the oxygen concentration in the oxygen concentration control box was 0-0.5% and then the NEC rats were quickly transferred into a refrigerator at 4˚C for 7 min for cold stimulation. After cold stimulation, 2 mg/kg LPS (2 mg/ml dissolved in normal saline) was intraperitoneally injected once a day for 3 consecutive days. Subsequently, suckling rats were returned to the incubator for rewarming and artificial feeding was continued. Hypoxia-cold stimulation was carried out every 12 h at 10 a.m. and 10 p.m., respectively, for 3 consecutive days. Rats in the control group were placed in the same cage, being suckled by the mother. All control rats were intraperitoneally injected with an equal amount of saline, once a day for 3 consecutive days. After 72 h, all rats were fasted for 12 h before being sacrificed with carbon dioxide euthanasia, and the volume displacement rate of CO_2 used for euthanasia ranged from 30-70% of the chamber volume per minute.

Adenovirus injection detection. Adenovirus was purchased from OBiO Technology (Shanghai) Corp., Ltd. Grouping of experimental animals and virus infection: The 14-day-old rats (weight 30-40 g) were randomly divided into two groups: i) control group (control, infected with NC virus group, NC group, n=5) and ii) intervention group (infected with TIPE2 over-expression virus, OE group, n=5). After being anesthetized with isoflurane (the induction dose used for anesthesia was 3-4% and the maintenance dose was 2.0-2.5%), SD rats of the two groups were injected with NC virus and OE

virus at multiple points in the ileum, respectively. Then the abdominal were closed and the rats were kept on normal feeding for 7 days. After 7 days, the rats were sacrificed with carbon dioxide euthanasia and the volume displacement rate of CO_2 used for euthanasia ranged from 30-70% of the chamber volume per minute. Then the ileum tissues were removed for further experiments. After the rats were injected with the virus, seven rats showed decreased activity, shortness of breath and finally succumbed due to respiratory arrest. It was suspected that the cause of their mortality may be viral intolerance.

Sample collection and processing. Midline laparotomies were performed on rats in a sterile environment. The intestinal tube between the lower end of the duodenum and the ileocecal was collected after isolating the mesentery and blood vessel. Subsequently, a 3-cm longitudinal section was made at the terminal ileum which was further divided into upper and lower segments. The upper segment was stored in 10% neutral formalin and the lower segment was snap-froze in liquid nitrogen and stored in -80˚C before experiment.

General observation. The general status of rats were observed and recorded on a daily basis. Detailed documentations of the changes were as previously described (17). During the modeling process, it was found that the general conditions of the rats in the model group were: No weight gain or loss, little activity or crouching immobility, low response to stimulation, feeding difficulties, diarrhea, black stool, and some rats exhibited bloody stool. The general morphology of intestinal tissues were evaluated after laparotomy and the presence of enteric cavity pneumatosis, necrosis, or hemorrhage was visually checked.

Hematoxylin and eosin (H&E) staining. The intestinal tissues were fixed in 10% neutral buffered formalin and embedded in a paraffin block (room temperature) before sectioning at 3 μm. After being dewaxing in xylene twice (at room temperature, 5-10 min each time), the sections were rehydrated at room temperature with an ethanol series (100, 95, 85 and 75%), for 3 min per gradient, and then soaked in distilled water for 2 min. The sections were stained with hematoxylin dye solution at room temperature for 20 min. The sections were differentiated with differentiation solution for 1 min at room temperature. The sections were then dehydrated, sealed with neutral gum and observed with an OLYMPUS BX53 light microscope (original magnification, x200).

Immunohistochemical (IHC) staining. Briefly, 3 μm sections were prepared for IHC staining. After deparaffinization and rehydration, the sections were put into a pressure cooker containing EDTA (pH 9.0) for antigen retrieval. Next, 3% hydrogen peroxide was added to inactivate endogenous peroxidase. Subsequently, the sections were successively incubated with the aforementioned primary and secondary antibodies and rinsed with PBS repeatedly. The primary antibody was added at 4˚C overnight, used at 1:500 dilution, and the horseradish peroxidase (HRP)-labeled secondary antibody (dilution, 1:500) was added at room temperature for 30 min. Finally, the nuclei were restained with hematoxylin for 1-2 min and then the tissue sections were sealed with neutral gum. Images of five non-overlapping fields per section were randomly taken using an OLYMPUS BX53 light microscope (original maginification, x200). The IHC staining and image analysis were carried out blindly.

Reverse transcription-quantitative polymerase chain reaction (RT-qPCR). Total RNA was extracted from tissue samples (<50 mg) using the Tissue RNA Purification Kit Plus according to the manufacturer's instructions. Purified RNA was reversely transcribed into cDNA using the Reverse Transcription System (Evo M-MLV Reverse transcription kit with gDNA Clean for qPCR II; Hunan Aikerui Biological Engineering Co., Ltd.) and the RT-qPCR was performed using the 2X Universal SYBR Green Fast qPCR Mix. Briefly, after an initial denaturation step at 95˚C for 3 min, the amplifications were carried out with 40 cycles at a melting temperature of 95˚C for 5 sec and an annealing temperature of 60˚C for 30 sec, followed by a melting curve analysis at 95˚C for 15 sec, 60˚C for 1 min and 95˚C for 1 sec. Data were collected by CFX Manager Software (Bio-Rad Laboratories, Inc.) and expressed as quantification cycle (Cq) values. The samples for RT-qPCR analysis were evaluated using a single predominant peak as quality control. The relative expressions of the target genes were calculated using the $2^{-\Delta\Delta Cq}$ method (18) and GAPDH and β-actin were adopted as the housekeeping gene. RNA extraction, cDNA synthesis and qPCR were performed according to the manufacturer's protocols, and all the experiments replicated three times. The primer sequences were as follows: TIPE2: Forward primer 5'-TCCAAGGCACAACGG GTGA-3' and reverse primer 5'-GGCGAAATCGTGTAGCCA GAG-3'; PI3K: Forward primer 5'-CAATCCAGAAACGCC TCACT-3'and reverse primer 5'-GCAGCCTCTATGGCAATC A-3'; AKT: Forward primer 5'-TACCTGAAGCTACTGGGC AAGGG-3' and reverse primer 5'-CGGTCGTGGGTCTGG AATGAG-3'; GAPDH (for the front experiments): Forward primer 5'-GCACCGTCAAGGCTGAGAAC-3' and reverse primer 5'-TGGTGAAGACGCCAGTGGA-3'; β-actin (for the later experiments): Forward primer 5'-CACCCGCGAGTA CAACCTTC-3' and reverse primer 5'-CCCATACCCACC ATCACACC-3'.

Western blotting analysis. The aforementioned TIPE2 was used at 1:1,000 dilution, and aforementioned HRP-conjugated secondary antibody (H+L) was used at 1:10,000 dilution. Total protein was extracted using lysis buffer containing 20 mmol/l Tris-HCl, pH 7.4, 150 mmol/l NaCl, 1% TX-100, 1 mmol/l EDTA, pH 8.0 and 1 mmol/l phenylmethylsulfonyl fluoride (PMSF). Protein concentration was determined using a Micro BCA protein kit (Pierce; Thermo Fisher Scientific, Inc.). Equal amounts of proteins (30 μg) were loaded on 10% gels to perform sodium dodecyl sulfate-polyacrylamide gel electrophoresis (SDS-PAGE) before transferring onto PVDF membranes. Membranes were blocked with 5% defatted milk in Tris-buffered saline (TBS) containing 0.1% Tween-20 at room temperature for 1 h and then incubated with primary antibodies including anti-TIPE2, anti-p-Akt, anti-Akt and anti-β-actin (ABclonal Biotech Co., Ltd.) and anti-PI3K and anti-p-PI3K (Abcepta) overnight at 4˚C. Subsequently, the blots were rinsed and

Table I. Weight changes of the two groups in 3 days.

Group	Number of rats	Weight, g			Weight change, g
		Day 1	Day 2	Day 3[a]	
Control	10	6.9±0.1	7.0±0.1	7.1±0.2	+0.2
NEC	10	6.6±0.6	6.4±0.6	6.2±0.6	-0.4

[a]P<0.05 vs. control group.

incubated with horseradish peroxidase (HRP)-conjugated secondary antibodies (room temperature, being rocked on a shaker for 1 h slowly). The immunoreactive bands were visualized using chemiluminescence ECL detection reagents (cat. no. BL520A; Biosharp Life Sciences) and actin was used as the loading control. ImageJ 1.51j8 software (National Institutes of Health) was used for analysis.

Statistical analysis. Data were shown as mean ± standard deviation (SD). The distribution was assessed with the Shapiro-Wilk test. Comparisons between two groups were performed using the unpaired t-test and a P-value <0.05 was considered statistically significant. Pearson's correlation analysis and linear regression analysis were performed with two variables (the index of TIPE2 and p-PI3K) in the NEC group, where TIPE2 was using as the independent variable and p-PI3K as the dependent variable. All statistical analyses were performed using the GraphPad Prism 8.0 (Dotmatics).

Results

Establishment of NEC rat model. At the beginning of modeling, the rats showed varying degrees of excretion of yellow-green mucus with diarrhea, dark belly, abdominal distension and weight loss, followed by vomiting, disappearance of group reaction, decreasing activity and sluggish reactions. These symptoms gradually aggravated. Table I showed the weight changes of the rats in the NEC group. The average body weight was significantly decreased in the NEC group compared to the control group (P<0.05).

Expression of TIPE2 was decreased in NEC rats. First, H&E staining was used to assess the ileocecal intestinal tissue damage. As shown in Fig. 1, rats in the NEC group presented with surface mucosal ulceration with necrosis. In addition, moderate or severe separations of submucosal and lamina propria commonly existed in the tissue, accompanied by moderate inflammatory cell infiltration and villi edema. Next, the expression of TIPE2 was examined by IHC staining. The immunoreactivity of TIPE2 was predominantly identified in infiltrating mononuclear cells in lamina propria and in epithelial cells to a lesser level. Fig. 2 showed the number of TIPE2-positive mononuclear cells in both groups.

Expressions of TIPE2, PI3K and AKT at mRNA level. RT-qPCR showed that the expression of TIPE2 mRNA was significantly reduced while the expressions of PI3K and AKT

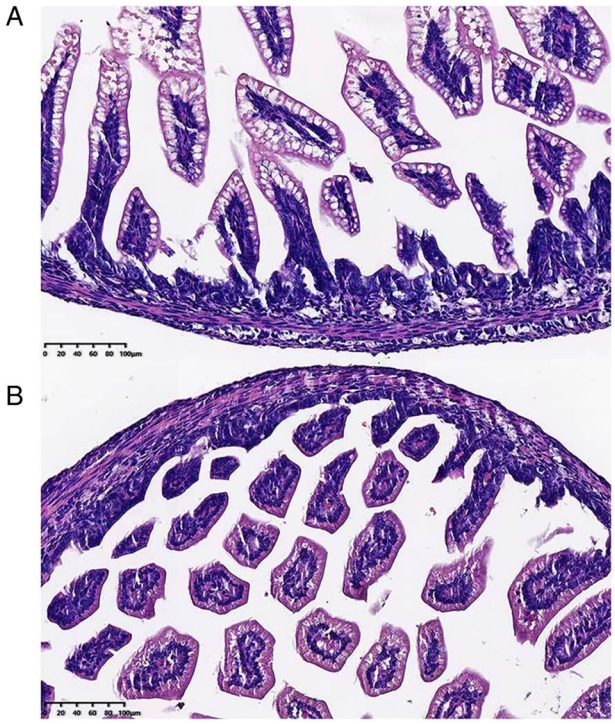

Figure 1. Hematoxylin and eosin staining of the intestinal mucosa morphology of the two groups. (A) The morphology of intestinal mucosa in the control group. (B) The morphology of intestinal mucosa in the necrotizing enterocolitis group: Intestinal tissue shows severe submucosal and lamina propria separation, with moderate inflammatory cell infiltration and villous edema. Scale bar, 100 μm.

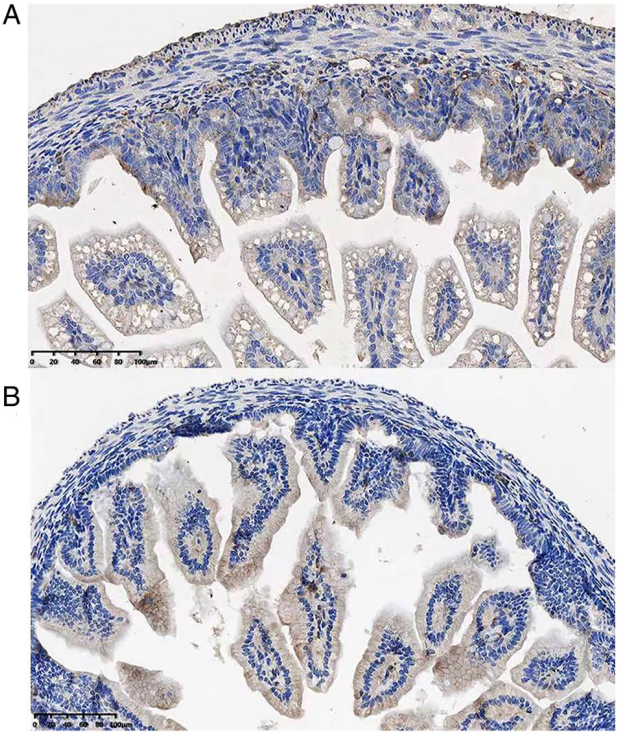

Figure 2. Expression of TIPE2 in the two groups by immunohistochemical staining. (A) Expression of TIPE2 in the control group. (B) Expression of TIPE2 in the necrotizing enterocolitis group: the immune activity of TIPE2 was predominant in infiltrating mononuclear cells in lamina propria. By observation, the number of TIPE2-positive mononuclear cells was significantly reduced in the necrotizing enterocolitis group compared with the control group. Scale bar, 100 μm. TIPE2, TNF-α-induced protein 8-like 2.

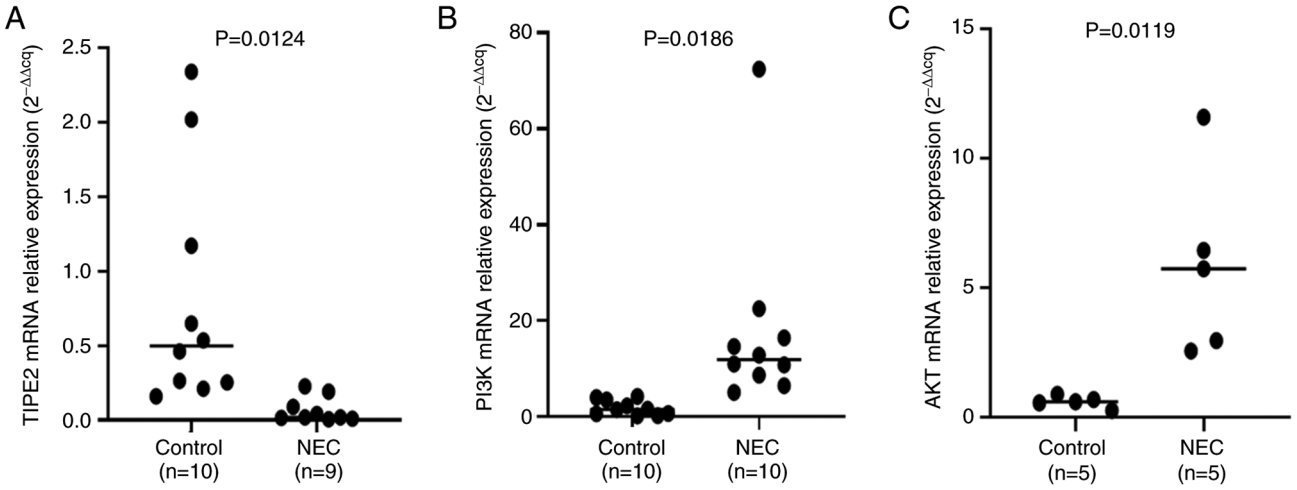

Figure 3. Comparison of relative expression of TIPE2, PI3K and AKT at mRNA level in NEC and the control group. The expression level of (A) TIPE2 mRNA, (B) PI3K mRNA and (C) AKT mRNA in NEC and the control groups. TIPE2, TNF-α-induced protein 8-like 2; PI3K, phosphatidylinositol-3-kinase; NEC, necrotizing enterocolitis.

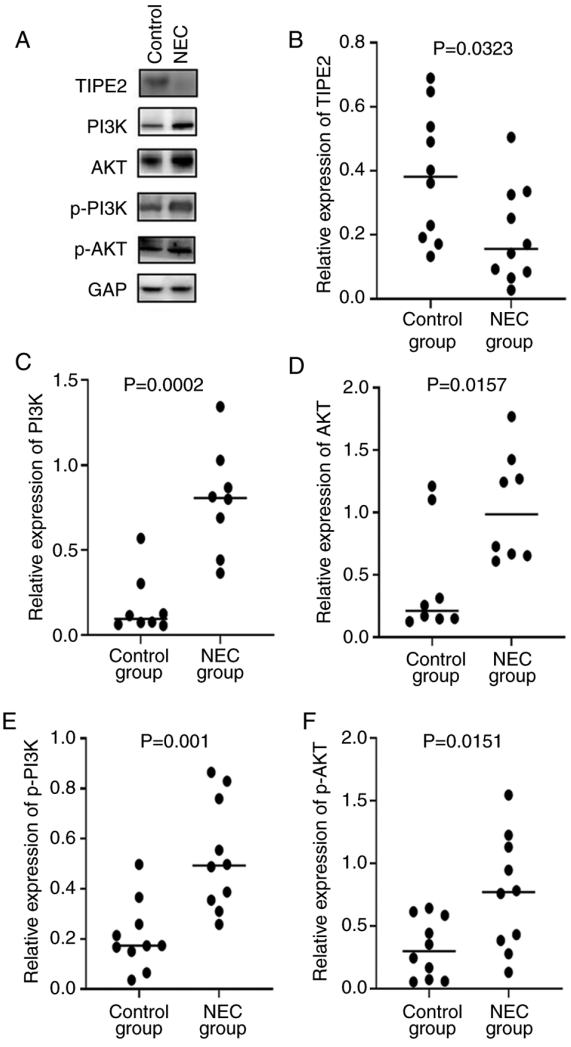

Figure 4. Expressions of TIPE2, pan-PI3K, pan-AKT, p-PI3K and P-AKT at the protein level. (A) Representative western blots of TIPE2, pan-PI3K, pan-AKT, p-PI3K and P-AKT expression in NEC rats and control groups. (B,C,D,E,F) The comparison of relative expression of (B) TIPE2, (C) pan-PI3K, (D) pan-AKT, (E) p-PI3K and (F) p-AKT in NEC rats and control groups. TIPE2, TNF-α-induced protein 8-like 2; PI3K, phosphatidylinositol-3-kinase; p-, phosphorylated; NEC, necrotizing enterocolitis.

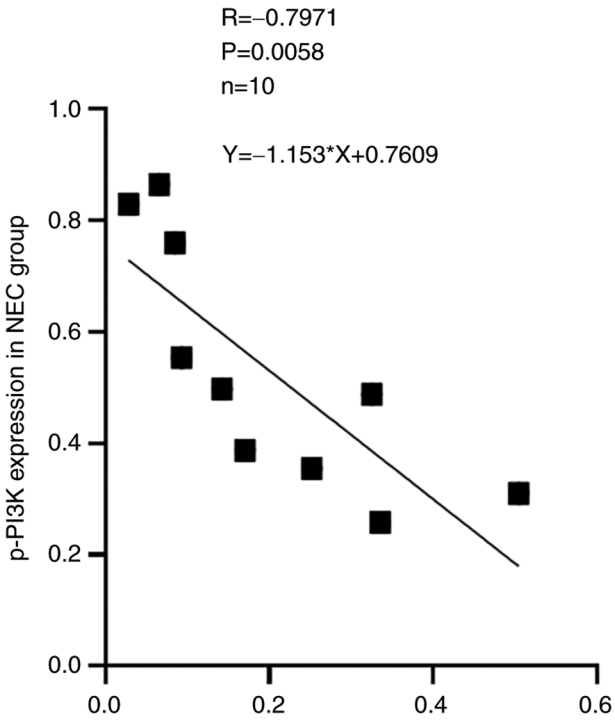

Figure 5. Relationship between TIPE2 and p-PI3K in the NEC group. From the linear regression analysis of TIPE2 and p-PI3K in the NEC group, TIPE2 was shown to be negatively correlated with p-PI3K (correlation coefficient: -0.7971). TIPE2, TNF-α-induced protein 8-like 2; PI3K, phosphatidylinositol-3-kinase; NEC, necrotizing enterocolitis.

were significantly increased in the NEC group compared to the control group (P<0.05). Fig. 3 showed the relative expression levels of TIPE2, PI3K and AKT.

Protein expressions of TIPE2, pan-PI3K, pan-AKT, p-PI3K and p-AKT. Western blotting analysis showed that the relative protein expression of TIPE2 in the NEC group was significantly decreased compared to the control group, while the relative expressions of p-PI3K, p-Akt, pan-PI3K and

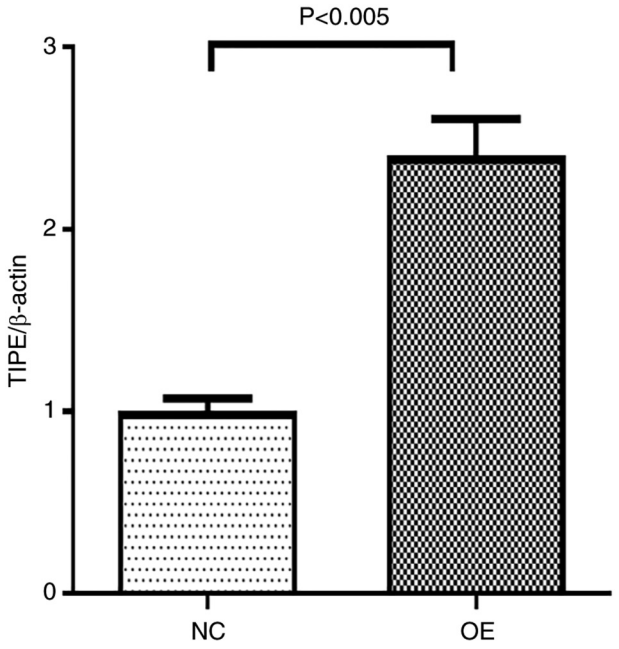

Figure 6. TIEP2 was significantly overexpressed in the OE group. TIPE2, TNF-α-induced protein 8-like 2; NC, negative control, a group of adenoviruses without TIPE2 overexpression; OE, TIPE2 overexpression group.

pan-Akt were significantly increased in the experimental group compared to the control group, as demonstrated by Fig. 4. Correlation analysis indicated that the protein expression of TIPE2 was negatively correlated with the expressions of p-PI3K with a coefficient factor of -0.797 (P=0.0058). Linear regression analysis of these two parameters showed that the regression coefficient factor was -1.153 (Fig. 5). This finding suggested that the TIPE2 might participate in the pathogenesis of NEC through regulating the PI3K/AKT signaling pathway.

Expression of the mRNA and major proteins of PI3K/AKT pathway in Ad-TIPE2-infected ileum. After adenovirus infection, TIPE2 expression in Ad-TIPE2-infected ileum was significantly increased, indicating successful infection Fig. 6. Then the follow-up experiments were conducted. Both RT-qPCR and western blot assay demonstrated that the expression of TIPE2 was significantly increased in Ad-TIPE2-infected ileum compared with Ad-V-infected ileum, while the expressions of PI3K and AKT at the mRNA and protein level in Ad-TIPE2-infected ileum were significantly decreased. And the differences of each index between the two groups were statistically significant (Figs. 7-9).

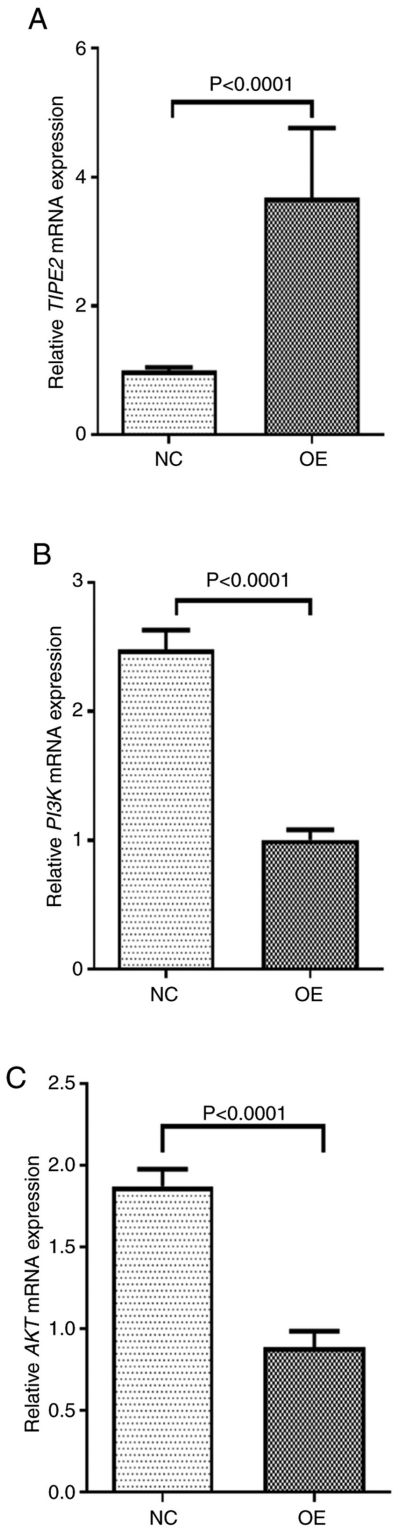

Figure 7. Comparison of TIPE2 mRNA, PI3K mRNA and AKT mRNA expression between Ad-TIPE2-infected group (OE) and Ad-V-infected group (NC). Relative expression of (A) TIPE2, (B) PI3K and (C) AKT at mRNA level in Ad-TIPE2-infected group and Ad-V-infected group. TIPE2, TNF-α-induced protein 8-like 2; PI3K, phosphatidylinositol-3-kinase; NC, negative control, a group of adenoviruses without TIPE2 overexpression; OE, TIPE2 overexpression group.

Discussion

To the best of the authors' knowledge, this was the first study that showed that the expression of TIPE2 at both mRNA and protein levels in a NEC rat model was decreased compared with a control group. Meanwhile, the expressions of PI3K and AKT at the mRNA level in the NEC group were significantly increased and the protein expressions of pan-PI3K, pan-Akt, p-PI3K and p-Akt in NEC rats were also significantly increased, compared to the controls. According to the correlation analysis, our data showed that the expression of TIPE2 was negatively correlated with the expression of p-PI3K(r =-0.797).

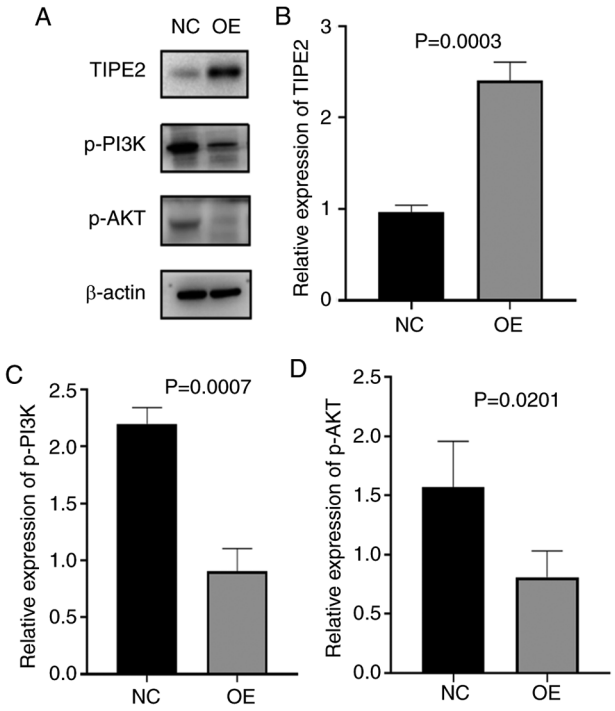

Figure 8. Expression of TIPE2, p-PI3K and p-AKT at the protein level. (A) The representative western blots of TIPE2, p-PI3K and p-AKT expression in Ad-TIPE2-infected group and Ad-V-infected group. The relative expression of (B) TIPE2, (C) p-PI3K and (D) p-AKT in Ad-TIPE2-infected group and Ad-V-infected group. TIPE2, TNF-α-induced protein 8-like 2; PI3K, phosphatidylinositol-3-kinase; p-, phosphorylated; NC, negative control, a group of adenoviruses without TIPE2 overexpression; OE, TIPE2 overexpression group.

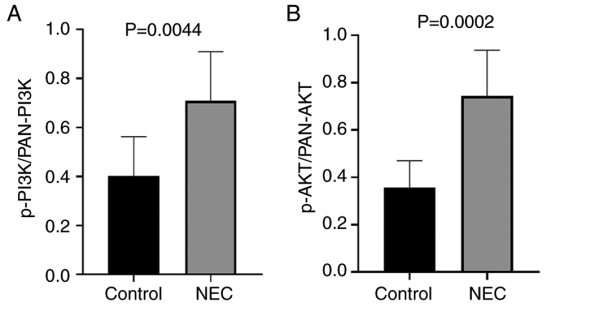

Figure 9. (A) Ratio of p-PI3K/PAN-PI3K. (B) Ratio of p-AKT/PAN-AKT. PI3K, phosphatidylinositol-3-kinase; p-, phosphorylated; NEC, necrotizing enterocolitis.

TIPE2 belongs to the TNF-α-induced protein 8 (TNFAIP8) family, which also includes members such as TNFAIP8, TIPE1 and TIPE3 (19). As aforementioned, TIPE2 has been identified as a tumor suppressor in multiple malignancies and its expression is significantly downregulated in a number of inflammatory and autoimmune diseases. TIPE2 over-expression can inhibit proliferation, epithelial-mesenchymal transition and migration. The depletion of TIPE2 can cause severe inflammatory and autoimmune diseases, such as hepatitis B, systemic lupus erythematosus, asthma, collagen-induced arthritis and experimental stroke (20-23). However, a previous study showed that TIPE2 deficiency could reduce inflammatory responses in a murine acute colitis model (11). Consistently, the present study found that the expression of TIPE2 was minimally expressed in NEC rat model. In other words, when NEC occurs in newborn rats, the body may reduce the expression of TIPE2 to prevent further activation of immune system to contain the inflammation.

PI3K and its downstream AKT both serve essential roles in regulating cell proliferation and survival as well as cell homeostasis (14). PI3K is an enzyme complex composed of 4 known isoforms (α,β,γ and ζ) and a catalytic p110 subunit. PI3K catalyzes the conversion of phosphatidylinositol 4,5 biphosphate PI(4,5)P3 to PI(3,4,5)P3. A number of proteins, such as phosphoinositide-dependent kinase-1 (PDK1), PDK2 and AKT, can interact with PI(3,4,5)P3. It has been known that PDK activates AKT by phosphorylation of Ser308 and Thr473 (13). Studies have reported that the PI3K/AKT signaling pathway serves a protective role in myocardial ischemic injury, rotavirus-induced diarrhea and fulminating polymicrobial sepsis (14,24,25). However, Camps *et al* (26) reported that blocking PI3Kγcould reduce inflammation and joint damage in murine models of arthritis. In addition, Oudit *et al* (27) found that PI3Kγ participates in the pathogenesis of maladaptive cardiac hypertrophy, whereas PI3Kα and βserve important roles in regulating physiologic stimuli that result in adaptive hypertrophy. Thus, different PI3K isoforms seem to serve significantly different roles under both physiological and pathological conditions. In the current study, mRNA expressions of PI3K and AKT as well as phosphorylation of PI3K and AKT were significantly increased in NEC rats. These results indicated that the PI3K/AKT pathway might be activated in NEC to reduce the inflammation and increase the susceptibility of rats to sepsis.

To further confirm the association between TIPE2 and PI3K/AKT pathway, wild type rats were infected with recombinant adenovirus Ad-V and Ad-TIPE2 respectively. The results showed that the expression of TIPE2 was significantly increased in Ad-TIPE2-infected rats, compared to controls. However, the phosphorylation of PI3K and AKT were significantly decreased in Ad-TIPE2-infected rats and the differences of each index between the two groups were statistically significant. All the data suggested that TIPE2 might be involved in the pathogenesis of NEC by activating the PI3K/AKT signaling pathway.

The data from the present study showed that TIPE2 was involved in the pathogenesis of NEC by activating the PI3K/Akt signaling pathway and its expression was downregulated in NEC rats. These findings not only provide an improved understanding of the pathogenesis of NEC but also shed light upon identifying novel therapeutic targets.

Acknowledgements

The authors would like to thank Dr Shun Wang (Department of Clinical Chemistry, The Second Hospital of Shandong University, Jinan, China), Dr Zhiyang Xiao (Editorial Department of Urology, The Second Hospital of Shandong University), Dr Lei Liu (Department of Urology, The Second Hospital of Shandong University), Dr Qian Xin (Department of Experimental Center, The Second Hospital

of Shandong University) and Dr Qinghong Ji (Obstetrical Department, The Second Hospital of Shandong University), for their help with the submission and the experiments.

Funding

The present study was supported by the Clinical Science and Technology Innovation Program of Ji Nan science and Technology Bureau funding (grant no. 201907088).

Availability of data and material

All data generated or analyzed during this study are included in this published article.

Authors' contributions

JL conceived and designed the present study, performed the experiments, collated the data and drafted the manuscript. RW made substantial contributions to conception and design, and reviewing and revising the manuscript critically for important intellectual content. SY was involved in drafting the manuscript, in data analysis and interpretation, and in revising it critically for important intellectual content. JX and XS contributed substantially to the experiments. JL and JX confirm the authenticity of all the raw data. All authors reviewed the manuscript for important intellectual content, agreed to be held accountable for all aspects of the work and read and approved the final manuscript.

Ethics approval and consent to participate

The present study was approved by the Animal Experiment Center of the Second Hospital of Shandong University (Shandong, China; approval no. KYLL-2022LW103).

Patient consent for publication

Not applicable.

Competing interests

The authors declare that they have no competing interests.

References

1. Huang L, Fan J, Chen YX and Wang JH: Inhibition of A_{2B} adenosine receptor attenuates intestinal injury in a rat model of necrotizing enterocolitis. Mediat Inflamm 2020: 1562973, 2020.
2. Jung K, Koh I, Kim JH, Cheong HS, Park T, Nam SH, Jung SM, Sio CA, Kim SY, Jung E, *et al*: RNA-seq for gene expression profiling of human necrotizing enterocolitis: A pilot study. J Korean Med Sci 32: 817-824, 2017.
3. Prencipe G, Auriti C, Inglese R, Gallusi G, Dotta A and De Benedetti F: The macrophage migration inhibitory factor-173g/c polymorphism is not significantly associated with necrotizing enterocolitis in preterm infants. J Pediatr Surg 48: 1499-1502, 2013.
4. Aceti A, Beghetti I, Martini S, Faldella G and Corvaglia L: Oxidative stress and necrotizing enterocolitis: Pathogenetic mechanisms, opportunities for intervention, and role of human milk. Oxid Med Cell Longev 2018: 7397659, 2018.
5. Fitzgibbons SC, Ching Y, Yu D, Carpenter J, Kenny M, Weldon C, Lillehei C, Valim C, Horbar JD and Jaksic T: Mortality of necrotizing enterocolitis expressed by birth weight categories. J Pediatr Surg 44: 1072-1075; discussion 1075-1076, 2009.
6. Martin CR and Walker WA: Probiotics: Role in pathophysiology and prevention in necrotizing enterocolitis. Semin Perinatol 32: 127-137, 2008.
7. Zhu Y, Tao M, Wu J, Meng Y, Xu C, Tian Y, Zhou X, Xiang J, Zhang H and Xie Y: Adenovirus-directed expression of TIPE2 suppresses gastric cancer growth via induction of apoptosis and inhibition of AKT and ERK1/2 signaling. Cancer Gene Ther 23: 98-106, 2016.
8. Liu ZJ, Liu HL, Zhou HC and Wang GC: TIPE2 inhibits hypoxia-induced Wnt/β-catenin pathway activation and EMT in glioma cells. Oncol Res 24: 255-261, 2016.
9. Wang Q, Ma L, Liu T, Ge C, Zhou Q, Wei C and Shi W: TIPE2 suppresses pseudomonas aeruginosa keratitis by inhibiting NF-κB signaling and the infiltration of inflammatory cells. J Infect Dis 220: 1008-1018, 2019.
10. Zhou J, Chen P, Li Z and Zuo Q: Gene delivery of TIPE2 attenuates collagen-induced arthritis by modulating inflammation. Int Immunopharmacol 79: 106044, 2020.
11. Lou Y, Sun H, Morrissey S, Porturas T, Liu S, Hua X and Chen YH: Critical roles of TIPE2 protein in murine experimental colitis. J Immunol 193: 1064-1070, 2014.
12. Fruman DA and Cantley LC: Phosphoinositide 3-kinase in immunological systems. Semin Immunol 14: 7-18, 2002.
13. Cantley LC: The phosphoinositide 3-kinase pathway. Science 296: 1655-1657, 2002.
14. Williams DL, Ozment-Skelton T and Li C: Modulation of the phosphoinositide 3-kinase signaling pathway alters host response to sepsis, inflammation, and ischemia/reperfusion injury. Shock 25: 432-439, 2006.
15. Hou Y, Lu X and Zhang Y: Irak inhibitor protects the intestinal tract of necrotizing enterocolitis by inhibiting the toll-like receptor (TLR) inflammatory signaling pathway in rats. Med Sci Monit 24: 3366-3373, 2018.
16. Auestad N, Korsak RA, Bergstrom JD and Edmond J: Milk-substitutes comparable to rat's milk; their preparation, composition and impact on development and metabolism in the artificially reared rat. Br J Nutr 61: 495-518,1989.
17. Yin Y, Liu F, Li Y, Tang R and Wang J: mRNA expression of TLR4, TLR9 and NF-κB in a neonatal murine model of necrotizing enterocolitis. Mol Med Rep 14: 1953-1956, 2016.
18. Livak KJ and Schmittgen TD: Analysis of relative gene expression data using real-time quantitative PCR and the 2 (-Delta Delta C(T)) method. Methods 25: 402-408, 2001.
19. Lou Y and Liu S: The TIPE (TNFAIP8) family in inflammation, immunity, and cancer. Mol Immunol 49: 4-7, 2011.
20. Xi W, Hu Y, Liu Y, Zhang J, Wang L, Lou Y, Qu Z, Cui J, Zhang G, Liang X, *et al*: Roles of TIPE2 in hepatitis B virus-induced hepatic inflammation in humans and mice. Mol Immunol 48:1203-1208, 2011.
21. Li F, Zhu X, Yang Y, Huang L and Xu J: Tipe2 alleviates systemic lupus erythematosus through regulating macrophage polarization. Cell Physiol Biochem 38: 330-339, 2016.
22. Ding J, Su J, Zhang L and Ma J: Crocetin activates Foxp3 through TIPE2 in asthma-associated treg cells. Cell Physiol Biochem 37: 2425-2433, 2015.
23. Zhang Y, Wei X, Liu L, Liu S, Wang Z, Zhang B, Fan B, Yang F, Huang S, Jiang F, *et al*: TIPE2, a novel regulator of immunity, protects against experimental stroke. J Biol Chem 287: 32546-32555, 2012.
24. Li HM, Li KY, Xing Y, Tang XX, Yang DM, Dai XM, Lu DX and Wang HD: Phenylephrine attenuated sepsis-induced cardiac inflammation and mitochondrial injury through an effect on the PI3K/Akt signaling pathway. J Cardiovasc Pharmacol 73: 186-194, 2019.
25. Zhang B, Wang Y, Jiang C, Wu C, Guo G, Chen X and Qiu S: Valeriana jatamansi Jones inhibits rotavirus-induced diarrhea via Phosphatidylinositol 3-Kinase/Protein Kinase B signaling pathway. J Microbiol Biotechnol 31: 1115-1122, 2021.
26. Camps M, Rückle T, Ji H, Ardissone V, Rintelen F, Shaw J, Ferrandi C, Chabert C, Gillieron C, Françon B, *et al*: Blockade of PI3Kgamma suppresses joint inflammation and damage in mouse models of rheumatoid arthritis. Nature Med 11: 936-943, 2005.
27. Oudit GY, Sun H, Kerfant BG, Crackower MA, Penninger JM and Backx PH: The role of phosphoinositide-3 kinase and PTEN in cardiovascular physiology and disease. J Mol Cell Cardiol 37: 449-471, 2004.